CD200 Expression Marks a Population of Quiescent Limbal Epithelial Stem Cells with Holoclone Forming Ability

SANJA BOJIC,[a] DEAN HALLAM,[a] NUNO ALCADA,[a] ALI GHAREEB,[a] RACHEL QUEEN,[a]
SAGOO PERVINDER,[b] HARLEY BUCK,[b] AYA AMITAI LANGE,[c] GUSTAVO FIGUEIREDO [ID],[a]
PAUL ROONEY,[d] MIODRAG STOJKOVIC,[e,f] ALEX SHORTT,[b] FRANCISCO C. FIGUEIREDO,[a,g]
MAJLINDA LAKO [ID][a]

Key Words. Cell surface markers • CD109 • CD200 • Limbal epithelial cells • Limbal stem cell •
Limbal stem cell deficiency • Quiescent stem cells

[a]Institute of Genetic Medicine, Newcastle University, Newcastle, United Kingdom; [b]UCL Institute of Immunology and Transplantation, London, United Kingdom; [c]Department of Genetics and Developmental Biology, The Ruth and Bruce Rappaport Faculty of Medicine, Technion - Israel Institute of Technology, Haifa, Israel; [d]Tissue Services, NHS Blood and Transplant, Liverpool, United Kingdom; [e]Faculty of Medical Sciences, Department of Genetics, University of Kragujevac, Serbia; [f]SPEBO Medical, Leskovac, Kragujevac, Serbia; [g]Department of Ophthalmology, Royal Victoria Infirmary, Newcastle University, Newcastle, United Kingdom

Correspondence: Majlinda Lako, Ph.D., Stem Cell Sciences, Newcastle University, Institute of Genetic Medicine and Institute for Ageing, International Centre for Life, Central Parkway, Newcastle upon Tyne NE1 3 BZ, United Kingdom. Telephone: 00 44191 2418688; e-mail: majlinda.lako@ncl.ac.uk

ABSTRACT

One of the main challenges in limbal stem cell (LSC) biology and transplantation is the lack of definitive cell surface markers which can be used to identify and enrich viable LSCs. In this study, expression of 361 cell surface proteins was assessed in ex vivo expanded limbal epithelial cells. One marker, CD200 was selected for further characterization based on expression in a small subset of limbal epithelial cells ($2.25 \pm 0.69\%$) and reduced expression through consecutive passaging and calcium induced differentiation. CD200 was localized to a small population of cells at the basal layer of the human and mouse limbal epithelium. CD200$^+$ cells were slow cycling and contained the majority of side population (SP) and all the holoclone forming progenitors. CD200$^+$ cells displayed higher expression of LSCs markers including *PAX6, WNT7A, CDH3, CK14, CK15,* and *ABCB5* and lower expression of *Ki67* when compared to CD200$^-$. Downregulation of *CD200* abrogated the ability of limbal epithelial cells to form holoclones, suggesting an important function for CD200 in the maintenance and/or self-renewal of LSCs. A second marker, CD109 which was expressed in $56.29 \pm 13.96\%$ of limbal epithelial cells, was also found to co-localize with ΔNp63 in both human and mouse cornea, albeit more abundantly than CD200. CD109 expression decreased slowly through calcium induced cell differentiation and CD109$^+$ cells were characterized by higher expression of Ki67, when compared to CD109$^-$ subpopulation. Together our data suggest that CD200 expression marks a quiescent population of LSCs with holoclone forming potential, while CD109 expression is associated with a proliferative progenitor phenotype. STEM CELLS 2018; 9999:1–13

SIGNIFICANCE STATEMENT

The cornea is the clear refractive window at the front of the eye that permits light to enter and be focused on the back of the eye. Stem cells in the cornea endlessly produce new cells to allow the window to remain clear and our eyes to function properly. A handful of proteins have been identified to mark the stem cells in the cornea, but this process results in loss of cellular viability. This study identified a novel cell surface marker, CD200, which enables enrichment of quiescent corneal stem cells with holoclone forming potential.

INTRODUCTION

The cornea is the transparent front part of the eye which together with the crystalline lens focuses the light onto retina for visual processing [1]. Corneal epithelial integrity and function is maintained by limbal stem cells (LSCs) which are found in a narrow peripheral region of the cornea, known as the limbus. Loss of LSCs results in a clinical condition called limbal stem cell deficiency (LSCD) characterized by chronic ocular surface inflammation, neovascularization, frequent stromal scarring, with consequent corneal opacity, pain, and loss of vision [2]. Transplantation of autologous ex vivo expanded LSCs from the healthy contralateral eye onto the patient's damaged eye is an established and European Medicines Agency authorized treatment for patients with total/ severe unilateral LSCD due to ocular surface burns [3]. Our group has developed good manufacturing practice (GMP) protocols for the ex vivo expansion of LSCs and has successfully transplanted 32 patients with unilateral

severe and total LSCD in phase I–II clinical trials [4]. Our method is based on the ex vivo expansion of a 1×2 mm^2 limbal biopsy cultured on human amniotic membrane resulting in the expansion of LSCs which migrate away from the explant and acquire the expression of differentiated epithelial markers resembling LSC migration and differentiation from the limbus toward the center of the cornea [5]. Using the same GMP protocols, we have also expanded ex vivo autologous oral mucosa epithelial cells which were used to successfully transplant two patients with bilateral LSCD [6]. Currently, ex vivo expansion strategies of limbal and other autologous epithelial stem cell are labor intensive and often lack standardization, largely because it is currently impossible to prospectively isolate pure populations of these cells for research or clinical use. Until this occurs, different centers will likely use specific techniques for isolation and ex vivo culture of LSCs in their respective institutions that have been developed and investigated in their individual basic laboratories, rendering it impossible to compare clinical success rates between clinical trials performed in different centers around the world.

An obvious problem with current clinical treatments is that transplanted cells are a heterogeneous cell population containing many cell types (ranging from epithelial, stromal stem and progenitor cells, conjunctival and corneal epithelial cells, and blood or vascular cells) in addition to LSCs, significantly affecting safety and efficiency of treatment. This was best highlighted by a landmark study published by Rama et al. who showed that successful corneal regeneration was strongly correlated with the presence of more than 3% holoclone-forming (ΔNp63α-bright) cells in ex vivo expanded cultures used for grafting of patients with LSCD [7]. Various studies have described morphological characteristics of LSCs (i.e., small cell size, pigmentation, and high nuclear to cytoplasmic ratio) [8], their slow cycling nature and location within clusters at palisades of Vogt [9]; however these factors have not been linked with LSC function and outcome of transplantation; hence harvesting a specific and purified sub-population of these cells remains a major challenge. Several key putative markers have already been identified including ΔNp63α, ABCG2, ABCB5, C/EBPσ, Bmi1, and Notch-1 among others [10–13]; however it is unclear whether these proteins are expressed by different LSC sub-populations or different LSC subsets within each population marked by a single putative marker.

Stem cell heterogeneity has been well described in various stem cell compartments including blood, skin, and intestinal epithelium pointing to the concomitant existence of multiple types of stem cells with distinct everyday roles [14]. From these studies, it has also emerged that these different stem cell types are more adaptable than previously thought, in that they have a "default" role under normal conditions, however following perturbation, such as stimulation by injury, they can fulfil distinct functions when required [14]. Some tissues may contain rapidly cycling, committed progenitors which are responsible for the majority of tissue maintenance, as well as a population of slow-cycling stem cells which maintain a higher degree of stemness and can act as alternative source of stem cells in response to injury and stress [15]. To date, it is not yet known whether corneal epithelium is also maintained by a combination of such quiescent and cycling progenitors, however it is interesting to note that in the human cornea two different sub-populations have been identified: (a) Bmi1$^+$,

C/EBPδ$^+$, and ΔNp63α$^+$ mitotically quiescent LSCs which generate holoclones in culture and (b) Bmi1$^-$, C/EBPδ$^-$, and ΔNp63α$^+$ population which respond to injury [16]. It is not known whether LSC heterogeneity extends beyond the presence of these two LSC sub-populations and whether cell surface markers to distinguish between these two subpopulations can be identified.

In this study, we used the LEGEND Screen Lyophilized Antibody Panel Human Cell Screening Kit to identify cell surface markers for human LSCs. Two markers, CD109 and CD200 were selected and studied in detail with respect to LSC proliferation, differentiation, and colony forming efficiency. Our data indicate that CD200 and CD109 expression mark quiescent LSC with holoclone forming potential and proliferative limbal epithelial progenitors respectively.

MATERIAL AND METHODS

Corneal Tissue

Cadaveric adult human limbal tissue was obtained from the corneo-scleral rings remaining (nine females, 15 males, average age 69.42 years, SEM 2.99, range 28–83 years) after removal of the central cornea for transplantation supplied by the NHS Blood and Transplant (NHSBT) Cornea Transplantation Service eye bank in Manchester and Bristol, UK. Average time from death to retrieval of corneo-scleral tissue was 16.1 ± 1.99 hours (mean ± SEM). Average time tissue spent in organ culture was 36.55 ± 7.8 days (mean ± SEM). Human tissue was handled according to the tenets of the Declaration of Helsinki and informed consent was obtained for research use of all human tissue from the next of kin of all deceased donors. The study was approved by the NRES Committee North East - Newcastle & North Tyneside 1 (REC number: 11/NE/0236, protocol number 5466) on the 29th October 2013.

Animal care and use conformed to the ARVO Statement for the Use of Animals in Ophthalmic and Vision Research. Immunostaining was performed on paraffin sections (5–7 μm) of C57BL/6 mouse tissues, as described previously [17].

Single Cell Culture of Human Limbal Epithelium on 3T3-J2 Feeder Layers

Twenty four hours before limbal epithelial cell isolation from corneo-scleral tissue, mitotically inactivated J2–3T3 mouse fibroblasts were suspended in high-glucose DMEM supplemented with bovine calf serum (10%) (Hyclone, Pittsburgh, USA) and penicillin/streptomycin (1%) (Thermo Fisher Scientific, Waltham, MA, USA) and plated in a 9.6 cm^2 tissue culture well at the final density of 2.4×10^4 cells per cm^2 as previously described [18]. The use of bovine calf serum instead of fetal calf serum was recommended by the manufacturer of the 3T3-J2 cell line (Karafast, New York, USA). The 3T3 cell suspension was placed in a tissue culture incubator at $37°$C overnight to allow the establishment of a 3T3 feeder layer. On the following day, LSCs were harvested from cadaveric corneo-scleral rims as previously described [19]. The deeper layers of the corneo-scleral rings were dissected away together with excess sclera leaving a ring containing approximately 2 mm of peripheral cornea and 2 mm of adjacent sclera. The remaining tissue containing limbal epithelium was then cut into smaller 1 mm^2

pieces. The limbal epithelial cells were isolated from these pieces using serial trypsinization with 0.05% trypsin–EDTA solution (Thermo Fisher Scientific, USA). After 20 minutes incubation in a tissue culture incubator, the resulting cell suspension was removed from the limbal pieces and epithelial medium was added to this suspension. After the cell suspension was centrifuged for 3 minutes at 1,000 rpm in Heraeus Megafuge 16R Centrifuge (Thermo Fisher Scientific, USA), the supernatant was removed and the remaining cell pellet was re-suspended in epithelial medium containing 3:1 mixture of low-glucose DMEM:F12 supplemented with fetal calf serum 10%, penicillin/streptomycin 1% (all Thermo Fisher Scientific, USA), hydrocortisone 0.4 µg/ml, insulin 5 µg/ml, triiodothyronine 1.4 ng/ml, adenine 24 µg/ml, cholera toxin 8.4 ng/ml, and EGF 10 ng/ml (all Sigma-Aldrich, Gilingham, UK). The trypsinization and centrifugation process was repeated a further three times using the same limbal tissue and the same centrifuge and settings. The resulting cell suspensions were pooled together. After counting, 30,000 of viable limbal epithelial cells (trypan blue exclusion test) in epithelial medium were added to one 9.6 cm^2 tissue culture well containing the growth arrested 3T3 fibroblast and placed in a tissue culture incubator at 37°C with a humidified atmosphere containing 5% CO_2. The medium was exchanged on the third culture day and every other day thereafter. After 3T3 feeder cells were detached and removed using 0.02% EDTA (Manchester, UK), sub-confluent primary cultures were dissociated with 0.5% trypsin–EDTA (Santa Cruz, California, USA) to single cell suspension and passaged at a density of 6×10^3 cells/cm^2. For serial propagation, cells were passaged and cultured as above, always at the stage of sub-confluence, until they reached passage 3.

Limbal Epithelial Cell Surface Marker Screening

Limbal epithelial cell cultures (passage 1) were dissociated as described above to a single cell suspension. Limbal epithelial cells were stained with 361 different phycoerythrin (PE) labeled antibodies and 10 immunoglobulin isotype controls using the LEGEND Screen Lyophilized Antibody Panel Human Cell Screening (PE) Kit (700007, BioLegend, San Diego, USA). After the staining, cells were washed and analyzed by LSR Fortessa (BD, USA) flow cytometer. Data were analyzed with FCS Express 6 Flow Cytometry Software (De Novo Software, Los Angeles, USA). The screening was repeated three times, for each experiment corneo-scleral rings from seven donors were pooled (21 donors in total; eight females, 13 males, average age 70.50 years, SEM 2.06, range 55–83 years).

Calcium Induced Differentiation

Limbal epithelial cells from three different donors (n = 3, passage 1) were plated at a density of 200,000 cells per well in a six well plate and cultured in EpiGRO Human Ocular Epithelia Complete Media Kit (SCMC001, Merck Millipore, New York, USA) without 3T3-J2 feeders or any plate coating. The medium contained basal medium, supplements mix (L-Glutamine 6 mM, Epinephrine 1.0 µM, Insulin 5 µg/ml, Apo-Transferrin 5 µg/ml, Hydrocortisone 100 ng/ml, EpiFactor O proprietary, and EpiFactor P 0.4%), 150 µM calcium and 1% penicillin/streptomycin. When the cells reached 80% confluence, calcium was added to a final concentration of 1.2 mM, for the induction of differentiation. Cells were differentiated for up to 1 week and collected for flow cytometry analysis.

Flow Cytometry Analysis and Fluorescence-Activated Cell Sorting

The expression of selected markers in limbal epithelial cell cultures was monitored through subsequent passages, from passage one to passage four, and during calcium induced differentiation using cells from three different donors (n = 3) to provide biological triplicates. After trypsin dissociation, limbal epithelial cells re-suspended in flow buffer (1% Bovine Serum Albumin in PBS) were stained for 20 minutes with different selected antibodies on ice and analyzed by flow cytometry (FACSCanto II, BD, North Carolina, USA). A minimum of 10,000 events were recorded for each sample. Antibodies used for fluorescence-activated cell sorting (FACS) were PE-conjugated anti-human CD200 (329205, BioLegend, USA, dilution factor 1:100), PE-conjugated anti-human CD109 (323305, BioLegend, USA, 1:100) and APC-conjugated anti-human p63 delta (NBP2-33090, Novus Biologicals, Abingdon, UK, USA, 1:100).

FACS was carried out using a FACSAria II sorter (BD, USA). Limbal epithelial cells used for the cell sorting experiments were passage 1. The limbal epithelial cell staining was performed as above using FACS buffer (1% FBS in PBS) under aseptic conditions for both final candidate markers, CD200 and CD109. The stained cell suspension was then filtered through a 40 µm nylon filter to remove any cell clumps. DAPI stain (10%) was added to a final cell suspension to eliminate dead cells. Side scatter and forward scatter profiles were used to eliminate cell doublets. Positive and negative sorted cells were used for colony-forming efficiency assay (CFE), clonal assay, and quantitative reverse transcriptase polymerase chain reaction (qRT-PCR).

CFE and Clonal Assay

CFE was performed as previously described by Yu et al. [18]. Following staining with 1% Rhodamine B, colonies were counted under dissecting microscope (SMZ645, Nikon, Tokyo, Japan). The CFE was calculated as number of colonies formed/number of cells plated $\times$ 100 for both positive and negative cell populations for three different donors (n = 3). Each donor served as a biological replicate. Sorted limbal epithelial cells from three different donors were also plated for clonal assay (n = 3) performed as described by Dziasko et al. [20]. Limbal epithelial cells used for the cell sorting experiments were passage 1. The sorted populations were re-plated for CFE and clonal assay. The clonal type was determined by (a) the morphology of colonies and (b) the percentage of aborted colonies as follows: when <5% of the total colonies were terminally differentiated, the clone was scored as a holoclone; when more than 95% of colonies were terminally differentiated, the clone was scored as a paraclone and finally, when >5% but <95% of colonies were terminally differentiated, the clone was classified as a meroclone [21, 22].

Fluorescence Immunocytochemistry and Microscopy

Cultured limbal epithelial cells, human frozen corneal sections and paraffin sections of mouse and human cornea were fixed for 15 minutes either in 4% paraformaldehyde (CD200 staining) or in ice-cold methanol (CD109 staining). A blocking step

was performed by incubation in antibody diluent containing 1% bovine serum albumin (Sigma-Aldrich, UK) with 5% normal goat serum (Thermo Fisher Scientific, USA) for 30 minutes prior to staining. Permeabilization with 0.2% Triton X-100 in PBS was performed prior to staining with antibodies for internal cell markers. Cells were incubated with primary antibodies at 4°C overnight and further incubated with secondary antibodies for 1 hour. The following primary antibodies were used at the indicated dilutions: anti CD109 (sc-271085, Santa Cruz, USA, 1:200), anti-human CD200 (329201, BioLegend, USA, 1:200), anti-mouse CD200 (AF3355, Novus Biologicals, USA, 1:100), anti p63 delta (NBP2-29467, Novus Biologicals, USA, 1:200), anti-cytokeratin 15 (ab52816, Abcam, Cambridge, UK, 1:100), and anti Ki67 antibody (ab15580, Abcam, UK, 1:100). Sections were mounted in Vecta shield (Vector Labs, Peterborough, USA) with Hoechst 33342 (1:1,000, Thermo Fisher Scientific, USA). Images were obtained using Axio Imager microscope with ApoTome accessory equipment and AxioVision software (Zeiss, Jena, Germany).

Quantitative Reverse Transcriptase Polymerase Chain Reaction

As in previous experiments, passage one of cultured limbal epithelial cells obtained from three different donors were used for the cell sorting ($n = 3$). The sorted cell populations were then subjected to qPCR analysis. cDNA was synthesized using the Cells-to-cDNA II kit (AM1723, Ambion, Thermo Fisher Scientific, USA) directly from cell lysates as per the manufacturer's protocol. Each reaction was set up using Go-Taq qPCR Master Mix (Cambridge, UK) and was composed of 5 μl X2 Master Mix buffer, 0.4 μl forward primer, 0.4 μl reverse primer, 0.8 μl template cDNA, 3.7 μl RNAse-free water, and 0.1 μl COX. All reactions were analyzed on a QuantStudio 7 Flex Real Time PCR System (Thermo Fisher Scientific, USA) according to the manufacturer's instructions using SYBR Green as the detection dye, and ROX channel to detect COX as the reference dye. A standard, 40-cycle qPCR was performed for each sample. The primer sequences used for qRT-PCR are listed in Supporting Information Table S1. The data was analyzed using the $2^{-\Delta\Delta Ct}$ calculation method.

Cell Proliferation Assay

Passage one of limbal epithelial cells from three different donors ($n = 3$) at 60%–70% confluence were exposed to BrdU at a final concentration of 10 μM in cell culture medium and incubated for 1, 4, and 8 hours. Control cells were cultured without BrdU. After incubation, cells were stained with PE conjugated anti-CD200 antibody (329205, BioLegend, USA) for 20 minutes on ice, then were washed, fixed, and permeabilized before DNAse treatment. Following BrdU epitope exposure cells were stained with PerCP-Cy5.5 conjugated anti-BrdU antibody (560809, BD, USA, 5 μl per test) and DAPI stain for cell cycle analysis and analyzed by LSR Fortessa (BD, USA) cell analyser.

Hoechst 33342 and Pyronin Y Staining for G0/G1 Separation

Quiescent cells, which are arrested in G0 phase, have lower level of RNA compared to active cells (G1 phase). Hoechst is an exclusive DNA dye while Pyronin Y reacts with both DNA and RNA. However, in the presence of Hoechst, Pyronin Y

reaction with DNA is blocked, and Pyronin Y stains RNA only. When cells are stained first with Hoechst 33342 and then with Pyronin Y it is possible to distinguish DNA from RNA. Limbal epithelial cells from three different donors ($n = 3$) were stained with APC conjugated anti-CD200 antibody for 20 minutes (329207, BioLegend, USA). For the separation of G0 and G1 cell cycle phases, limbal epithelial cells were stained with Hoechst 33342 (Sigma-Aldrich, UK) in a final concentration 10 μg/ml and incubated at 37°C for 45 minutes. After 45 minutes, 5 μl of 100 μg/ml Pyronin Y (Sigma-Aldrich, UK) was added directly to the cells and incubated at 37°C for a further 15 minutes. Single color controls and negative control were also prepared. LSR Fortessa (BD, USA) flow cytometer was used to analyze cells.

Small Interfering RNA Transfection

To investigate the impact of *CD200* downregulation on the clonal ability of limbal epithelial cells, RNA interference (RNAi) was performed using small interfering RNA (siRNA). Passage one human limbal epithelial cells from three different donors were grown on 3T3 feeder layer in complete epithelial medium supplemented with EGF, adenine, cholera toxin, hydrocortisone, insulin, and triiodothyronine. A day before transfection, limbal epithelial cells (150×10^3) were re-seeded in 12-well plate without feeders in order to increase transfection efficiency. The day after re-seeding cells were transfected with CD200 Human Stealth siRNAs (set of three: HSS106678, HSS106679, HSS181160; 1299003, Thermo Fisher) and Stealth RNAi siRNA Negative Control Lo GC (12935200, Thermo Fisher) using Lipofectamine RNAiMAX Transfection Reagent (13778030, Thermo Fisher) according to the manufacturer's protocol. The transfected cells were incubated for 48 hours for CFE and clonal assay.

After 48 hours incubation with CD200 siRNA and control siRNA, cells we re-seeded back to six well plates in different densities (500 and 1,000 cells/well) and cultured on 3T3 feeders for next 14 days. The rest of the cells were used for RNA extraction and qRT-PCR to confirm *CD200* downregulation.

Statistical Analysis

GraphPadPrism 7.0 (San Diego, CA, https://www.graphpad.com/scien-tific-software/prism/) was used to perform all statistical analyses. The data showed normal distribution therefore Student's *t* test was used to analyze differences between groups and $p \leq .05$ was considered statistically significant. All experiments were performed in biological replicates of three or more, and data are presented as mean ± SEM.

RESULTS

Flow Cytometric Based Cell Surface Screening of Limbal Epithelial Cell Cultures

After removing 3T3 feeder cells with EDTA, passage one subconfluent limbal epithelial cells were lifted from the tissue culture plates using Trypsin–EDTA and stained with 361 human surface proteins and analyzed by flow cytometry. The cell surface marker screening was performed three times and in each case, limbal epithelial cells from seven different donors were pooled to obtain sufficient cell number for this type of

analysis. A summary of these results is shown in Supporting Information Table S2. LEGEND Screen analysis confirmed high expression of the commonly cited limbal epithelial cell markers: EGFR (88.81 $\pm$ 6.02) [8, 23, 24], SSEA-4 (54.02 $\pm$ 5.93%) [25], CD71 (88.76 $\pm$ 5.92) [8, 26], integrin $\beta 5$ (91.45 $\pm$ 1.24) [27], integrin $\alpha 6$ (92.54 $\pm$ 6.41) [26], E-cadherin (88.48 $\pm$ 6.06) [11] as well as many other general markers of corneal epithelium. The presence of other markers previously related to limbal epithelial cells was also confirmed: CD40 (26.00 $\pm$ 6.94) [28], CD117 (c-kit) (8.22 $\pm$ 2.56) [29, 30], CD146 (67.04 $\pm$ 2.87), and CD166 (95.08 $\pm$ 0.97) [30] as well as the presence of putative LSC marker integrin $\alpha 9/\beta 1$ (4.85 $\pm$ 1.98) [8, 11, 24, 30, 31]. The expression of the autophagy marker LAMP1 (84.82 $\pm$ 11.89) was also high, corroborating with previously reported data on limbal epithelial cultures [32].

Marker selection for further investigation was based on three criteria: (a) presence in a small subpopulation of cells (up to 10%) in accordance with label retaining cells in the limbal zone making up less than 10% of the total population (assessed on the basis of the percentage of radiolabeled thymidine retaining cells present in the limbal zone [33]) and the studies of Umemoto and co-workers showing that approximately 10% of total limbal epithelial cells expressed the putative LSC marker ABCG2 [34]; (b) passage or calcium differentiation induced reduction in expression frequency in limbal epithelial cells; and (c) presence in other epithelial stem or progenitor cells. CD200 (2.25 $\pm$ 0.69%, n = 3) was one of the few markers that fulfilled all these three criteria [35–38] and was selected for further characterization. In addition to LSC markers, we also selected putative transient amplifying cell surface markers based on similar expression to ΔNp63 (assessed by our group to be expressed in 45%–60% of ex vivo expanded limbal epithelial cells [18]) as well as passage and differentiation induced reduction in expression frequency in limbal epithelial cells. CD109 (56.29 $\pm$ 13.96%, n = 3) was among the cell surface marker that fulfilled these criteria and was selected for further characterization.

The Expression of CD109 in Human Limbal Epithelial Cell Cultures, Human, and Murine Corneas

The LEGEND Screen results were confirmed by flow cytometric analysis which showed CD109 to be expressed in a relatively high percentage of limbal epithelial cultures in p1 (47.51 $\pm$ 9.35%, n = 5) (Fig. 1A). The expression of CD109 did not vary significantly through the first four passages (p > .05) (Fig. 1A). Nonetheless, the expression of CD109 decreased significantly (p < .05) after 5 days of calcium-induced differentiation under feeder-free conditions similarly to ΔNp63 expression (p < .05) (Fig. 1B).

Using immunostaining, we determined the localization of CD109$^+$ cells in human ocular surface epithelial tissues (Fig. 1C). CD109$^+$ cells were exclusively located at the limbus and co-localized with ΔNp63 (Fig. 1C), while undetectable in the suprabasal and superficial layers of limbal epithelium as well as in the all layers of central corneal epithelium (Fig. 1C). In murine corneal tissue, CD109 (Fig. 1D) was also exclusively located at the limbus and co-localized with ΔNp63 and CK15 while absent in central corneal epithelium. In vitro, CD109$^+$cells were present predominantly on the outer border of colonies (Fig. 1E).

Colony Forming Efficiency and Proliferative Ability of CD109$^+$ Cells

To identify actively replicating cells, and thereby assess cellular proliferation, BrdU was applied to cells in culture and the number of cells in the S phase was monitored after 1, 4, and 8 hours incubation with BrdU by flow cytometry. No statistically significant differences were found in the percentage of cells in the S phase of the cell cycle for CD109$^+$ or CD109$^-$ population after incubation with BrdU for 1 and 4 hours. However, after 8 hours incubation with BrdU, there was a significantly higher number of CD109$^+$ cells in the S phase compared do CD109$^-$ cells (Fig. 1F: p = .0073, Supporting Information Fig. S1D).

Sorted positive and negative cells for both markers were tested for their colony forming efficiency and clonal potency (n = 3). There were no significant differences between the positive and negative cells in CFE (Fig. 1H); however the relative colony-covered-area size was significantly greater in CD109$^+$cells (p < .01), meaning they formed larger colonies (Fig. 1G, 1I) when compared to CD109$^-$ cells. Despite the fact that both CD109$^+$ and CD109$^-$ cells formed colonies classified as meroclones, number of aborted colonies was significantly higher (p = .0047) in CD109$^-$ population (Fig. 1J, 1K).

The Expression of CD200 in Human Limbal Epithelial Cell Cultures, Human, and Murine Corneas

CD200 was expressed in a small percentage of limbal epithelial cultures in p1 (4.13 $\pm$ 1.10%, n = 10) (Fig. 2A). Furthermore, the expression of CD200 decreased significantly (p < .05) and rapidly through subsequent passages (Fig. 2A). During calcium induced differentiation, the expression of CD200 disappeared from the culture after 5 days (p < .05) (Fig. 2B). For all the markers, including CD109, CD200, and ΔNp63, a lower expression was observed under feeder-free culture conditions used for the calcium-induced differentiation assays, which may suggest that the feeder-free culture is less conducive to LSC maintenance.

The presence of CD200$^+$ cells was confirmed in the basal layer of the limbal epithelium, while its expression was absent in all the other layers of limbal and corneal epithelium (Fig. 2C). In murine corneal tissue, CD200 (Fig. 2D) was exclusively located at the limbus and co-localized with ΔNp63 and CK15 while absent in other parts of corneal epithelium. CD200$^+$ cells were also present in ex vivo expanded limbal epithelial cell cultures, but in lower number compared to CD109$^+$ cells and moreover were found scattered throughout the colonies (Fig. 2E). CD200$^+$ cells (3.66 $\pm$ 0.25%) were much less abundant than ΔNp63$^+$ cells (47.65 $\pm$ 3.01%) (Fig. 2E, Supporting Information Fig. S1A). All CD200$^+$ cells were also ΔNp63$^+$; however ΔNp63$^+$ CD200$^+$ cells represented only 6.23 $\pm$ 0.97% of all ΔNp63$^+$ cells (Supporting Information Fig. S1B).

Colony Forming Efficiency and Proliferative Ability of CD200$^+$ Cells

The proliferative potential of CD200$^+$ cells was examined by Ki67 immunofluorescent staining of limbal epithelial cells cultured in vitro (Fig. 2F). Interestingly, while some CD200$^+$cells were Ki67$^+$ (41.67 $\pm$ 0.22%), there were more Ki67$^-$ cells in the CD200$^+$ population (58.33 $\pm$ 0.22%) (Supporting Information Fig. S1C).

There were no statistically significant differences in CFE between CD200$^+$ and CD200$^-$ groups (Fig. 3B), however CD200$^+$ cells were exclusively able to form holoclones—large
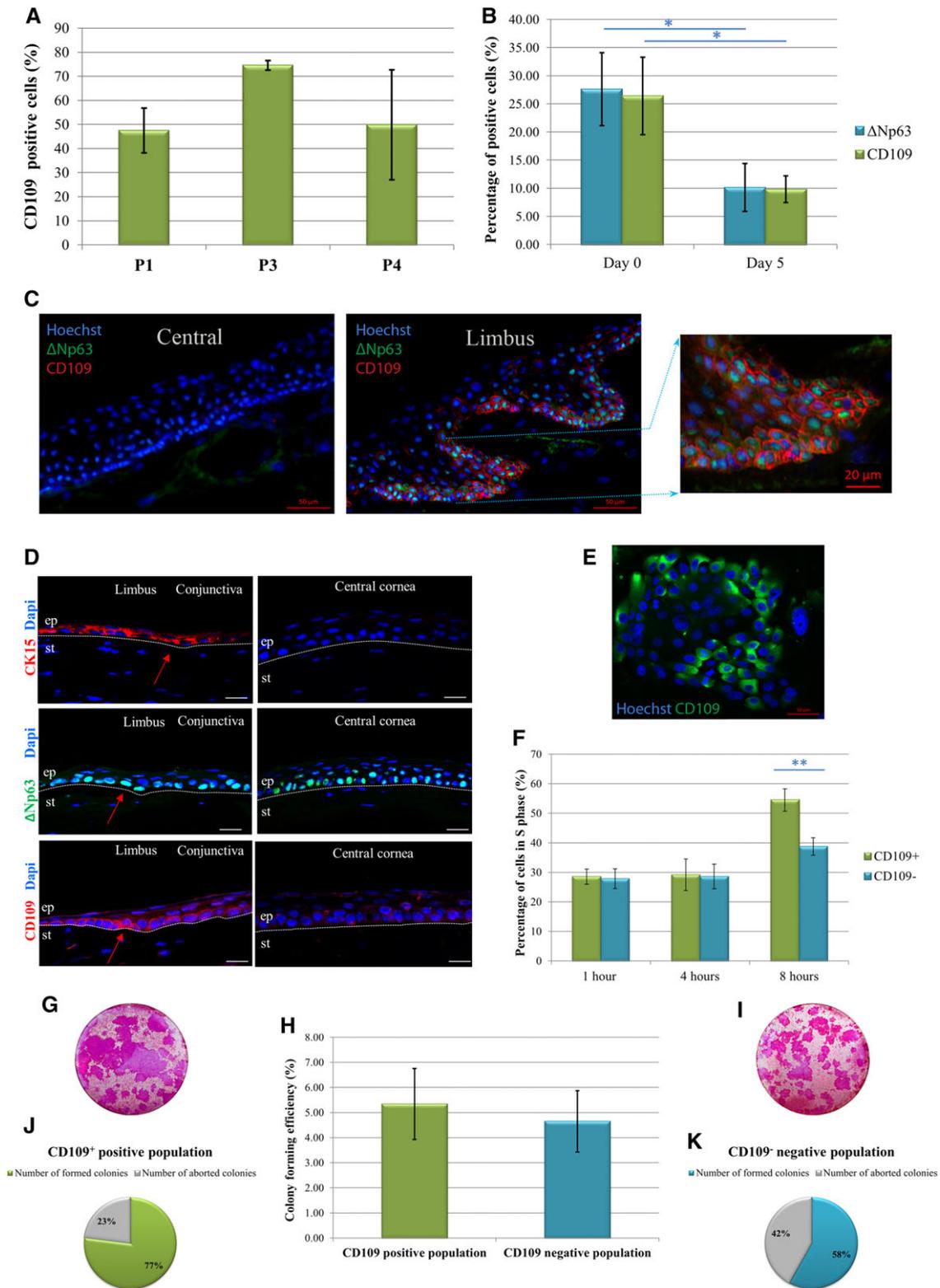
Figure 1. CD109 expression in human and mouse cornea in vivo and during ex vivo expansion of human limbal epithelial cells. **(A):** Quantification of CD109 expression through different passages of limbal epithelial cells by flow cytometry. Values represent mean ± SEM, n = 3–5 (n, number of biological replicates). **(B):** Quantification of ΔNp63 and CD109 expression during calcium induced differentiation of limbal epithelial cells by flow cytometry. Values represent mean ± SEM, n = 3, *, $p < .05$. **(C):** Immunohistochemical staining of human corneal tissue cryosections for ΔNp63 and CD109 within the central cornea and limbus. Nuclei are shown by Hoechst counter staining. Scale bars 50 μm with exception of additional inset with higher magnification with scale bar of 20 μm. **(D):** Immunohistochemical staining of murine corneal tissue cryosections for CK15, ΔNp63, and CD109 within the central cornea and limbus. Nuclei are shown by DAPI counter staining. The dashed line indicates the stromal-epithelial junction. Red arrows point at the limbal region. Scale bars 20 μm. **(E):** CD109

colonies with smooth, thick borders (Fig. 3D), while CD200⁻ cells formed meroclones which were characterized by irregular borders (Fig. 3E). The number of aborted colonies was significantly higher in CD200⁻ population ($p = .0061$). Using the percentage of terminal colonies described in the methods, CD200⁺ colonies were scored as holoclones (Fig. 3A) while CD200⁻ colonies were scored as meroclones (Fig. 3C).

CD200⁺ cells were slow to enter S phase: at 1 and 4 hours there were significantly less CD200⁺ in S phase when compared to CD200⁻; these differences became non-significant at 8 hours (Fig. 3F, 3G). For that reason we used Hoechst 33342 and Pyronin Y staining for G0/G1 separation. A larger part of G0 subpopulation was made up by CD200⁺ cells ($59.30 \pm 3.12\%$) than CD200⁻ cells ($40.70 \pm 2.11\%$; Fig. 3H). Interestingly, we also found that majority ($78.66 \pm 3.20\%$) of SP cells were in the CD200⁺ population (Supporting Information Fig. S1E) while the CD200⁻ population contained less SP cells ($21.34 \pm 3.20\%$; Fig. 3I).

The Expression of LSC Markers in the CD109 and CD200 Positive and Negative Populations

To investigate the transcriptional profile of CD109⁺ and CD200⁺ cells, expression of putative LSC markers *ΔNp63*, *ABCB5*, *C/EBPδ*, *BMI1*, *AXIN2*, *FZD7*, *CHD3*, *WNT7A*, *CK14*, and *CK15* [12, 16, 39–43], corneal epithelial differentiation marker *CK3* [44] and marker of proliferative cells *Ki67* [45] was assessed by qRT-PCR.

The expression of *CD109*, was significantly higher ($p < .01$) in CD109⁺ group compared to CD109⁻ group, thus validating the flow activated cell sorting strategy. In addition, the expression of LSC markers *PAX6* ($p < .05$) and C*K14* ($p < .01$) and proliferative marker *Ki67* ($p < .001$) was also higher in the CD109⁺ group when compared to the CD109⁻ (Fig. 4A). No statistically significant differences were found in the expression of other LSC markers *ΔNp63*, *ABCB5*, *C/EBPδ*, *BMI1*, *AXIN2*, *FZD7*, *CHD3*, *WNT7A*, and C*K15* and corneal differentiation marker *CK3* between the CD109⁺ and CD109⁻ group (Fig. 4A).

CD200 was significantly upregulated in CD200⁺ cell population ($p < .001$) along with the putative LSC markers *ABCB5* ($p < .001$), *CDH3* ($p < .001$), *PAX6* ($p < .01$), *WNT7A* ($p < .01$), *CK14* ($p < .01$), and C*K15* ($p < .001$). On the other hand, *ΔNp63* and *Ki67* ($p < .05$) were significantly downregulated in CD200⁺ cell population compared to the CD200⁻ cell population. There were no significant differences in the expressions of *C/EBPδ*, *BMI1*, *AXIN2*, *FZD7*, and *CK3* between the CD200⁺ and CD200⁻ groups (Fig. 4B).

CD200 siRNA Transfection

To investigate the impacts of *CD200* downregulation on limbal epithelial cell cultures, RNAi was carried out using a pool of three different siRNAs as detailed in the materials and methods section. Quantitative RT-PCR analysis confirmed downregulation of *CD200* in the group treated with *CD200* siRNA compared to control group ($p < .05$) (Fig. 5A).

Interestingly, the colony forming efficiency assay showed no significant difference in the percentage of formed paraclones or meroclones between the two groups (Fig. 5B, 5C), but holoclones completely disappeared from the siRNA transfected group (Fig. 5C, 5D), leading to a significant difference of the percentage of holoclones formed between the groups ($p < .05$).

DISCUSSION

LSCs are tissue-specific stem cells with a high proliferative potential and self-renewal capacity responsible for the life-long maintenance of corneal tissue in both homeostasis and wound repair [11, 46, 47]. To date, a few putative LSC markers (e.g., ΔNp63, ABCG2, C/EBPδ, BMI1, PAX6, WNT7A, ABCB5) have been associated with LSCs, however, among these, only ABCB5 represents a cell surface marker that enables enrichment of viable LSCs. In this study, we used the LEGEND Screen Lyophilized Antibody Panel to assess the expression of 361 cell surface markers in ex vivo expanded limbal epithelial stem cells and selected CD200 and CD109 as cell surface markers of interest for further investigation.

Up to date, there are no reports of either CD109 or CD200 expression or functional significance in the corneal epithelium. CD109 is a glycosylphosphatidylinositol–anchored glycoprotein whose expression is upregulated in several types of human cancers, particularly squamous cell carcinomas, while in normal human tissues CD109 expression is limited to certain cell types including myoepithelial cells of mammary, lacrimal, salivary, and bronchial glands, basal cells of the prostate and bronchial epithelium [48], human hepatic progenitor cells [49], endothelial cells and a subpopulation of bone marrow CD34⁺ cells enriched in hematopoietic stem and progenitor cells [50]. CD109 has been shown to enhance EGF-signaling in the SK-MG-1 glioblastoma cell line through the interaction of membrane anchored N-terminal CD109 fragment with EGFR [51], and to negatively regulate TGF-β1 signaling in keratinocytes by either directly modulating receptor activity or by binding of soluble CD109 to type I TGF-β receptor [52, 53]. TGF-β is an important cytokine that negatively regulates proliferation of different cell types including primary cultured human limbal epithelial cells [54]. Mii et al. reported that CD109-deficient mice exhibit epidermal hyperplasia and chronic skin inflammation, and CD109 regulates differentiation of keratinocytes in vivo [48]. Taken together these data show that the CD109 molecule plays an important role in epithelial cell proliferation through the positive regulation of EGF and negative regulation of TGF-β signaling as well as being involved in epithelial cell differentiation.

Our results showed that CD109 is expressed in both human and mouse corneal epithelium and is co-localized with ΔNp63 in the basal layer of the limbal epithelium while is

---

immunohistochemical staining of human limbal epithelial colony in vitro. Nuclei are shown by Hoechst counter staining. Scale bar 50 μm. **(F):** Quantification of cells in the S phase of the cell cycle in CD109⁺ and CD109⁻ population after 1, 4, and 8 hours incubation with BrdU. Values represent mean $\pm$ SEM, $n = 3$, **, $p < .001$. **(G):** Colonies of CD109⁺ limbal epithelial cells stained with 2% rhodamine. **(H):** Comparison of colony forming efficiency between CD109⁺ and CD109⁻ cell populations. Values represent mean $\pm$ SEM, $n = 3–5$. **(I):** Colonies of CD109⁻ limbal epithelial cells stained with 2% rhodamine. **(J):** Pie chart showing the distribution of formed and aborted colonies in CD109⁺ population. **(K):** Pie chart showing the distribution of formed and aborted colonies in CD109⁻ population. Abbreviations: ep, epithelium; st, stroma.
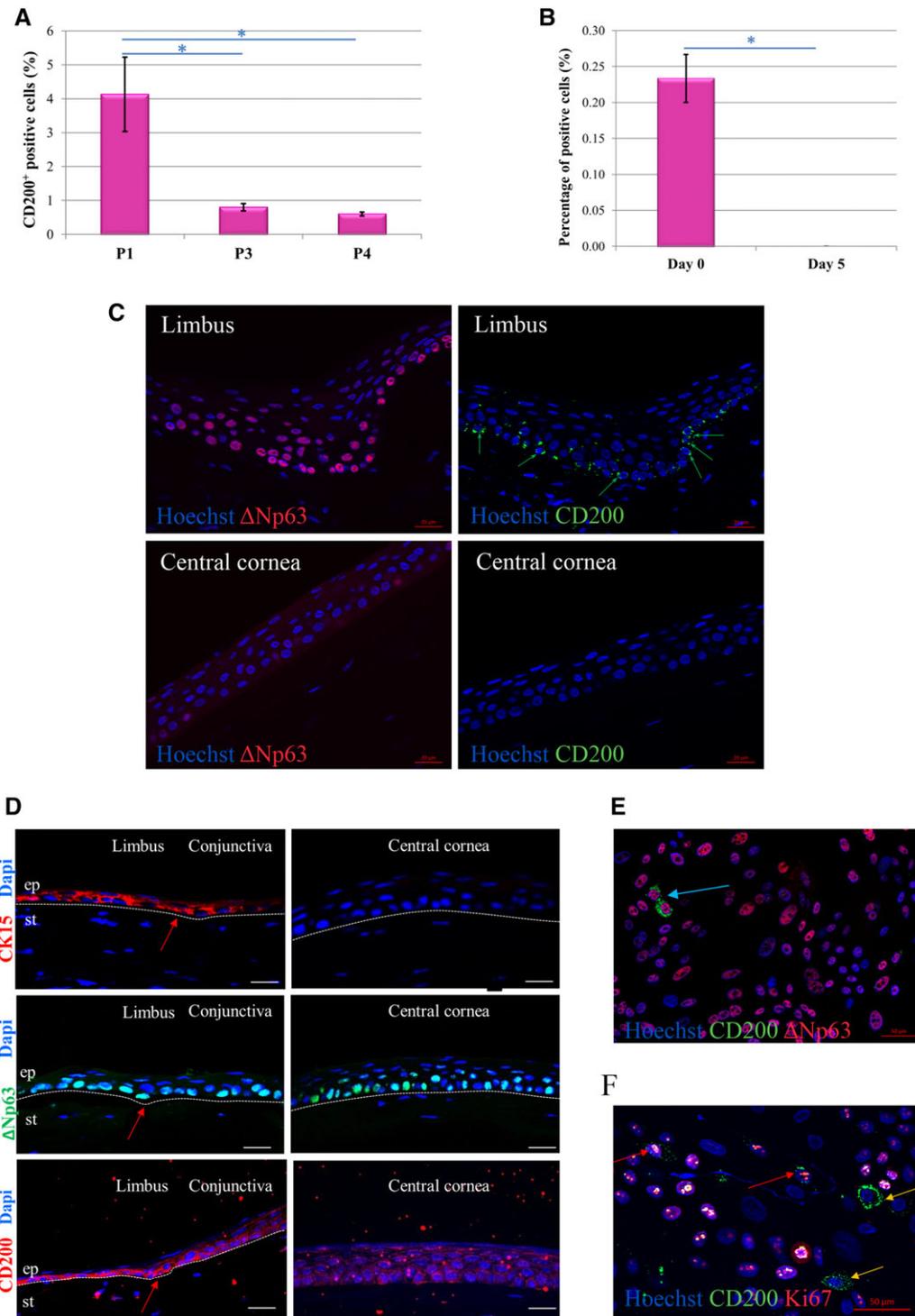
Figure 2. CD200 expression in human and mouse cornea in vivo and during ex vivo expansion of human limbal epithelial cells. **(A):** Quantification of CD200 expression through different passages of limbal epithelial cells by flow cytometry. Values represent mean $\pm$ SEM, n = 3–10 (n, number of biological replicates), *, $p < .05$. **(B):** Quantification of CD200 expression during calcium induced differentiation of limbal epithelial cells by flow cytometry. Values represent mean $\pm$ SEM, n = 3, *, $p < .05$. **(C):** Immunohistochemical staining of human corneal tissue paraffin sections for ΔNp63 and CD200 within the central cornea and limbus. Nuclei are shown by Hoechst counter staining. Scale bars 20 μm. **(D):** Immunohistochemical staining of murine corneal tissue cryosections for CK15, ΔNp63, and CD200 within the central cornea and limbus. Nuclei are shown by DAPI counter staining. The dashed line indicates the stromal-epithelial junction. Red arrows point at limbal region. Scale bars 20 μm. **(E):** Immunohistochemical staining of limbal epithelial cell colonies in vitro for CD200 and ΔNp63. Blue arrow points CD200$^+$ cells. Nuclei are shown by Hoechst counter staining. Scale bar 50 μm. **(F):** Immunohistochemical staining of limbal epithelial cell colonies in vitro for CD200 and Ki67. Red arrows point to CD200$^+$ Ki67$^+$ cells; orange arrows point to CD200$^+$Ki67$^-$ cells. Nuclei are shown by Hoechst counter staining. Scale bar 50 μm. Abbreviations: ep, epithelium; st, stroma.
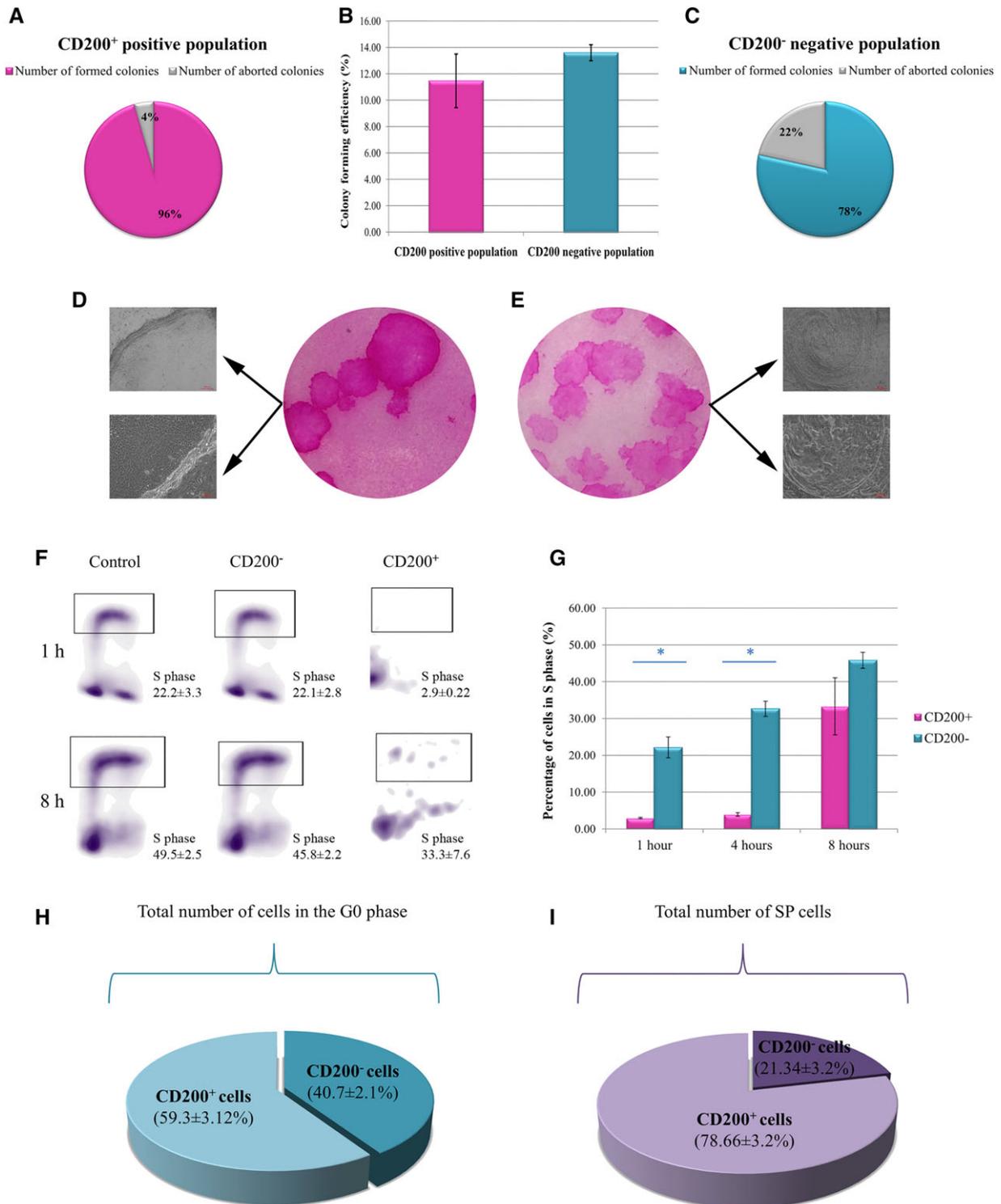
Figure 3. Colony forming efficiency and proliferative potential of sorted CD200 positive and negative population. **(A):** Pie chart showing the distribution of formed and aborted colonies in CD200$^+$ population. **(B):** Comparison of colony forming efficiencies of CD200$^+$ and CD200$^-$ cells. Values represent mean ± SEM, n = 3 (n, number of biological replicates). **(C):** Pie chart showing the distribution of formed and aborted colonies in CD200$^-$ population. Values represent mean ± SEM, n = 3. **(D):** Microscopic and macroscopic appearances of colonies formed by CD200$^+$ cells. Scale bars 100 μm. **(E):** Microscopic and macroscopic appearances of colonies formed by CD200$^-$ cells. Scale bars 100 μm. **(F):** BrdU cell proliferation assay of CD200 negative and positive limbal epithelial cell population after 1- and 8-hours incubation with BrdU. Values represent mean ± SEM, n = 3.**(G):** Quantification of cells in the S phase of the cell cycle in CD200$^+$ and CD200$^-$ population after 1, 4, and 8 hours incubation with BrdU. Values represent mean ± SEM, n = 3, *, $p < .05$. **(H):** The contribution of CD200$^+$ and CD200$^-$ cell population to the total number of cells in the G0 phase of the cell cycle. Values represent mean ± SEM, n = 3. **(I):** The contribution of CD200$^+$ and CD200$^-$ cell population to the total number of side population cells. Values represent mean ± SEM, n = 3.
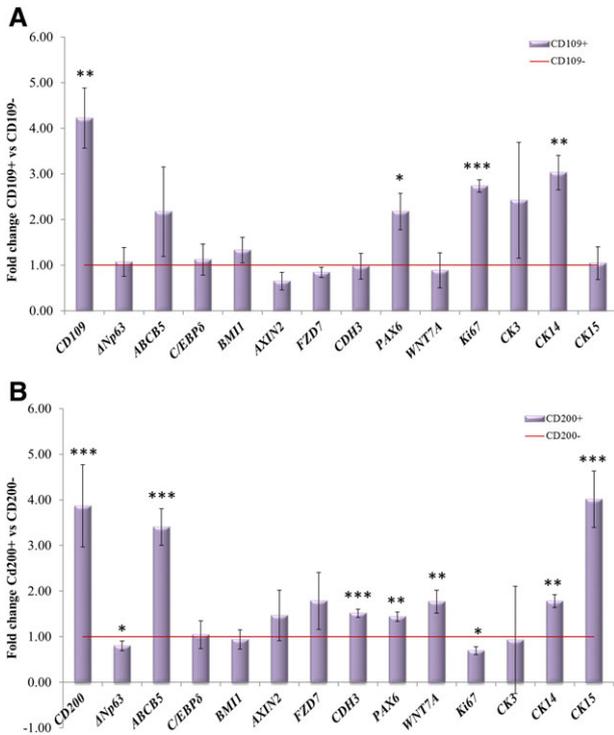
Figure 4. Expression of putative limbal stem cell and corneal epithelial cell markers in the sorted CD109 and CD200 positive and negative cell populations. **(A):** Quantitative reverse transcriptase polymerase chain reaction expression data for CD109^{+} limbal epithelial cell population versus CD109^{−} limbal epithelial cell population represented by the red line (value 1). Values represent mean ± SEM, $n = 3$ (n, number of biological replicates), *, $p < .05$; **, $p < .01$; ***, $p < .001$. **(B):** Quantitative reverse transcriptase polymerase chain reaction expression data for CD200^{+} limbal epithelial cell population versus CD200^{−} limbal epithelial cell population represented by the red line (value 1). Values represent mean ± SEM, $n = 3$, *, $p < .05$; **, $p < .01$; ***, $p < .001$.

absent in the other layers of the limbal epithelium and all layers of the central corneal epithelium. In vitro, CD109^{+} cells were located at the edge of growing colonies, similar to ΔNp63 expression in proliferating cells at the periphery of holoclones as previously reported [55]. Moreover, CD109 expression decreased during calcium-induced differentiation in a similar manner to ΔNp63 expression. There were more CD109^{+} cells in S phase of the cells cycle after 8 hours incubation with BrdU. This observation together with the higher Ki67 expression and larger colony area formed by the CD109^{+} cells suggest that CD109 represents a cell surface marker for proliferating corneal epithelial progenitor cells.

Previous studies have suggested the presence of a stem cell niche at the bulge region of the hair follicle, which contains CD200^{+} cells [35, 37, 38, 56, 57] and have shown enrichment of human bulge stem cells by positive selection using CD200 as a cell surface marker [58]. CD200 (also known as OX-2) is a transmembrane glycoprotein that transmits an immunoregulatory signal through its receptor (CD200R) to attenuate inflammatory reactions and promote immune tolerance [37]. CD200/CD200R mediated intracellular communication among different epidermal cell sub-populations may have an important role in preventing undesired immune responses in the

skin [59]. Hair follicles represent one of the few sites of "immune privilege" [60], possibly with the aim of preserving keratinocyte stem cells [61]. The CD200 molecule therefore may play a vital role in this "protection" since CD200/CD200R interaction attenuates perifollicular inflammation and prevents hair follicle specific autoimmunity, thereby protecting the epidermal stem cell reservoir from autoimmune destruction [62]. Additionally, CD200 has a clinical importance in allo- and xeno-transplantation [63]. CD200 overexpression in transgenic mice increases skin, cardiac, and renal allograft survival [64] by suppression of inflammation and acquired immunity. Apart from normal tissues, high CD200 expression was found in colon cancer, myeloma, breast and brain cancer, melanoma and normal mesenchymal stem cells [65]. It is closely related to tumor immunosuppression and has been proposed as a cancer stem cell marker in colon cancer [65]. CD200 has also been proposed as a putative marker of corneal endothelial cells that enables their differentiation from stromal keratocytes and corneal stromal fibroblasts [66]. We also observed CD200^{+} corneal endothelial cells in human corneal sections corroborating data published by Cheong et al. [66] (data not shown).
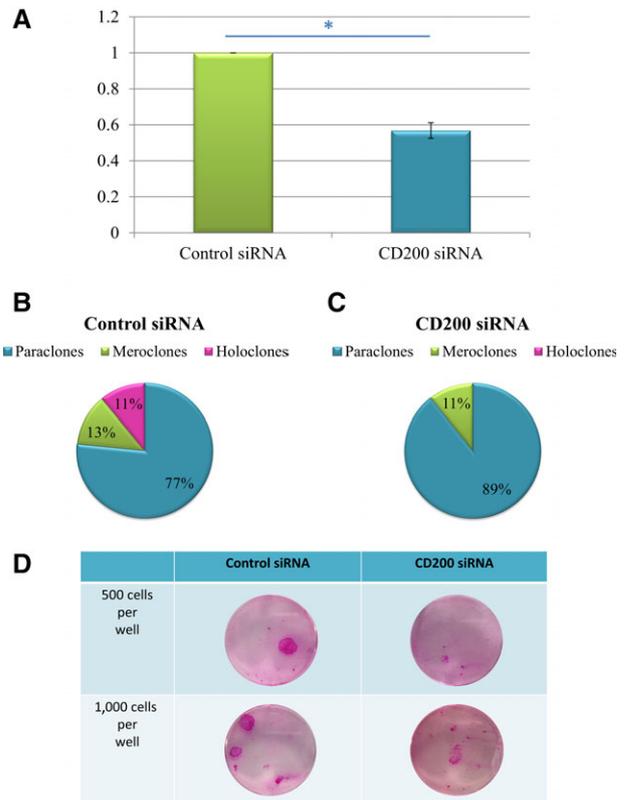

Figure 5. CD200 knockdown and its effect on clonal ability of limbal epithelial cells. **(A):** Quantitative reverse transcriptase polymerase chain reaction expression data for control siRNA versus CD200 siRNA treated limbal epithelial cells. Values represent mean ± SEM, $n = 3$ (n, number of biological replicates), *, $p < .05$. **(B):** Pie chart showing distribution of paraclones, meroclones, and holoclones formed by control siRNA treated cells and **(C):** CD200 siRNA treated cells. **(D):** Representative images of colonies formed in control and CD200 siRNA group, with 500 or 1,000 cells seeded per well. Abbreviation: siRNA, small interfering RNA.

Taking into consideration this published literature and the low frequency of CD200^{+} in our limbal epithelial cultures (<5%), we hypothesized that CD200 may represent a potential cell surface marker of LSCs. Using immunostaining in human and mouse corneal tissue, we showed that CD200 is exclusively located at the base of the limbal epithelium. In addition, its expression is significantly and rapidly decreased upon subsequent passaging and calcium induced differentiation of limbal epithelial cells in keeping with a stem/transient amplifying cell phenotype. CD200^{+} cells obtained from hair follicle have been shown to possess a high CFE potential [35]; however our findings do not support these results. We found no significant difference between the CFE of CD200 positive and negative populations. However, we showed that only CD200^{+} cells were able to form holoclones which are derived from LSCs, while CD200^{−} cells produced meroclones which are known to descend from transient amplifying cells. Moreover, we showed that CD200^{+} cells are slow cycling and only start to enter the S phase of the cells cycle after 8 hours long incubation with BrdU, whereas CD200^{−} cells enter the S phase 1 hour after incubation with BrdU. Importantly, downregulation of *CD200* by RNAi led to complete loss of holoclones, thus indicating an important role for CD200 in the maintenance and /or self-renewal of LSCs from which the holoclones are derived.

Both quiescent and active stem cell subpopulations coexist in several tissues, in separate yet adjoining locations [15]. We observed a higher number of Ki67^{−} cells and lower expression of *Ki67* within the CD200^{+} population when compared to CD200^{−} cells, suggesting that CD200^{+} may represent the quiescent LSCs. Indeed, a larger part of cells in G0 phase was made up with CD200^{+} cell population which in itself contained 79% of the SP cells, corroborating previously published findings by Umemoto et al. that limbal epithelial SP are quiescent and do not

demonstrate proliferative capabilities in ex vivo culture conditions [67]. We also observed a consistently higher expression of putative LSC markers including *WNT7A*, *PAX6*, *ABCB5*, *CDH3*, *CK14*, and *CK15* [12, 42, 43, 55, 68–71] in the CD200^{+} subpopulation.

In summary, we report herein the identification of a new cell surface marker for LSCs (CD200) as well as a cell surface marker for proliferating progenitor cells (CD109). We believe that the identification of these two new cell surface markers will significantly aid live enrichment of these two cell types and their biological and clinical applications with potential benefits for patients suffering with LSCD.

AUTHOR CONTRIBUTIONS

S.B.: experimental conception and design, collection and assembly of data, data analysis and interpretation, manuscript writing, final approval of manuscript; D.H., N.A., A.G., S.P., H.B., A.A.L., G.F., P.R., M.S., and A.S.: collection and/or assembly of data, final approval of manuscript; F.C.F.: conception and design, fund raising, final approval of manuscript; M.L.: study conception and design, fund raising, data analysis, manuscript writing, final approval of manuscript.

REFERENCES

1 Osei-Bempong C, Figueiredo FC, Lako M. The limbal epithelium of the eye—A review of limbal stem cell biology, disease and treatment. BioEssays 2013;35:211–219.

2 Baylis O, Rooney P, Figueiredo F et al. An investigation of donor and culture parameters which influence epithelial outgrowths from cultured human cadaveric limbal explants. J Cell Physiol 2013;228:1025–1030.

3 European Medicines Agency. Holoclar. Available at http://www.ema.europa.eu/ema/index.jsp?curl=pages/medicines/human/medicines/002450/human_med_001844.jsp&mid=WC0b01ac058001d124. Accessed April 5, 2018.

4 Kolli S, Ahmad S, Lako M et al. Successful clinical implementation of corneal epithelial stem cell therapy for treatment of unilateral limbal stem cell deficiency. Stem Cells (Dayton, Ohio). 2010;28:597–610.

5 Kolli S, Lako M, Figueiredo F et al. Loss of corneal epithelial stem cell properties in outgrowths from human limbal explants cultured on intact amniotic membrane. Regen Med 2008;3:329–342.

6 Kolli S, Ahmad S, Mudhar HS et al. Successful application of ex vivo expanded human autologous oral mucosal epithelium for the treatment of total bilateral limbal stem cell deficiency. Stem Cells (Dayton, Ohio). 2014;32:2135–2146.

7 Rama P, Matuska S, Paganoni G et al. Limbal stem-cell therapy and long-term corneal regeneration. N Engl J Med 2010;363: 147–155.

8 Chen Z, de Paiva CS, Luo L et al. Characterization of putative stem cell phenotype in human limbal epithelia. Stem Cells (Dayton, Ohio) 2004;22:355–366.

9 Dua HS, Shanmuganathan VA, Powell-Richards AO et al. Limbal epithelial crypts: A novel anatomical structure and a putative limbal stem cell niche. Br J Ophthalmol 2005; 89:529–532.

10 Pellegrini G, Dellambra E, Golisano O et al. p63 identifies keratinocyte stem cells. Proc Natl Acad Sci USA 2001;98:3156–3161.

11 Schlotzer-Schrehardt U, Kruse FE. Identification and characterization of limbal stem cells. Exp Eye Res 2005;81:247–264.

12 Ksander BR, Kolovou PE, Wilson BJ et al. ABCB5 is a limbal stem cell gene required for corneal development and repair. Nature 2014;511:353–357.

13 Joe AW, Yeung SN. Concise review: Identifying limbal stem cells: Classical concepts and new challenges. Stem Cells Translational Medicine 2014;3:318–322.

14 Goodell MA, Nguyen H, Shroyer N. Somatic stem cell heterogeneity: Diversity in the blood, skin and intestinal stem cell compartments. Nat Rev Mol Cell Biol 2015;16: 299–309.

15 Li L, Clevers H. Coexistence of quiescent and active adult stem cells in mammals. Science 2010;327:542–545.

16 Barbaro V, Testa A, Di Iorio E et al. C/EBPdelta regulates cell cycle and self-renewal of human limbal stem cells. J Cell Biol 2007;177:1037–1049.

17 Nasser W, Amitai-Lange A, Soteriou D et al. Corneal-committed cells restore the stem cell pool and tissue boundary following injury. Cell Rep 2018;22:323–331.

18 Yu M, Bojic S, Figueiredo GS et al. An important role for adenine, cholera toxin, hydrocortisone and triiodothyronine in the proliferation, self-renewal and differentiation of limbal stem cells in vitro. Exp Eye Res 2016;152:113–122.

19 Ahmad S, Stewart R, Yung S et al. Differentiation of human embryonic stem cells into corneal epithelial-like cells by in vitro

replication of the corneal epithelial stem cell niche. Stem Cells (Dayton, Ohio) 2007;25: 1145–1155.

20   Dziasko MA, Armer HE, Levis HJ et al. Localisation of epithelial cells capable of holoclone formation in vitro and direct interaction with stromal cells in the native human limbal crypt. PLoS One 2014;9:e94283.

21   Pellegrini G, Golisano O, Paterna P et al. Location and clonal analysis of stem cells and their differentiated progeny in the human ocular surface. J Cell Biol 1999;145:769–782.

22   Barrandon Y, Morgan JR, Mulligan RC et al. Restoration of growth potential in paraclones of human keratinocytes by a viral oncogene. Proc Natl Acad Sci USA 1989;86: 4102–4106.

23   Zieske JD, Wasson M. Regional variation in distribution of EGF receptor in developing and adult corneal epithelium. J Cell Sci 1993; 106Pt 1:145–152.

24   Kim HS, Jun Song X, de Paiva CS et al. Phenotypic characterization of human corneal epithelial cells expanded ex vivo from limbal explant and single cell cultures. Exp Eye Res 2004;79:41–49.

25   Truong TT, Huynh K, Nakatsu MN et al. SSEA4 is a potential negative marker for the enrichment of human corneal epithelial stem/progenitor cells. Invest Ophthalmol Vis Sci 2011;52:6315–6320.

26   Hayashi R, Yamato M, Saito T et al. Enrichment of corneal epithelial stem/progenitor cells using cell surface markers, integrin alpha6 and CD71. Biochem Biophys Res Commun 2008;367:256–263.

27   Stepp MA, Spurr-Michaud S, Gipson IK. Integrins in the wounded and unwounded stratified squamous epithelium of the cornea. Invest Ophthalmol Vis Sci 1993;34: 1829–1844.

28   Iwata M, Soya K, Sawa M et al. CD40 expression in normal human cornea and regulation of CD40 in cultured human corneal epithelial and stromal cells. Invest Ophthalmol Vis Sci 2002;43:348–357.

29   Luznik Z, Hawlina M, Malicev E et al. Effect of cryopreserved amniotic membrane orientation on the expression of limbal mesenchymal and epithelial stem cell markers in prolonged limbal explant cultures. PLoS One 2016;11:e0164408.

30   Albert R, Vereb Z, Csomos K et al. Cultivation and characterization of cornea limbal epithelial stem cells on lens capsule in animal material-free medium. PLoS One 2012;7: e47187.

31   Jones PH, Watt FM. Separation of human epidermal stem cells from transit amplifying cells on the basis of differences in integrin function and expression. Cell 1993;73: 713–724.

32   Dhamodaran K, Subramani M, Jeyabalan N et al. Characterization of ex vivo cultured limbal, conjunctival, and oral mucosal cells: A comparative study with implications in transplantation medicine. Mol Vis 2015;21:828–845.

33   Cotsarelis G, Cheng SZ, Dong G et al. Existence of slow-cycling limbal epithelial basal cells that can be preferentially stimulated to proliferate: Implications on epithelial stem cells. Cell 1989;57:201–209.

34   Umemoto T, Yamato M, Nishida K et al. Rat limbal epithelial side population cells exhibit a distinct expression of stem cell markers that are lacking in side population cells from the central cornea. FEBS Lett 2005; 579:6569–6574.

35   Ohyama M, Terunuma A, Tock CL et al. Characterization and isolation of stem cell-enriched human hair follicle bulge cells. J Clin Invest 2006;116:249–260.

36   Ohyama M. Hair follicle bulge: A fascinating reservoir of epithelial stem cells. J Dermatol Sci 2007;46:81–89.

37   Rosenblum MD, Olasz EB, Yancey KB et al. Expression of CD200 on epithelial cells of the murine hair follicle: A role in tissue-specific immune tolerance? J Invest Dermatol 2004;123:880–887.

38   Gerhards NM, Sayar BS, Origgi FC et al. Stem cell-associated marker expression in canine hair follicles. J Histochem Cytochem 2016;64:190–204.

39   Figueira EC, Di Girolamo N, Coroneo MT et al. The phenotype of limbal epithelial stem cells. Invest Ophthalmol Vis Sci 2007;48: 144–156.

40   Kalha S, Shrestha B, Sanz Navarro M et al. Bmi1+ progenitor cell dynamics in murine cornea during homeostasis and wound healing. 2018;36:562–573.

41   Mei H, Nakatsu MN, Baclagon ER et al. Frizzled 7 maintains the undifferentiated state of human limbal stem/progenitor cells. Stem Cells (Dayton, Ohio). 2014;32:938–945.

42   Sartaj R, Zhang C, Wan P et al. Characterization of slow cycling corneal limbal epithelial cells identifies putative stem cell markers. Sci Rep 2017;7:3793.

43   Yoshida S, Shimmura S, Kawakita T et al. Cytokeratin 15 can be used to identify the limbal phenotype in normal and diseased ocular surfaces. Invest Ophthalmol Vis Sci 2006;47:4780–4786.

44   Merjava S, Neuwirth A, Tanzerova M et al. The spectrum of cytokeratins expressed in the adult human cornea, limbus and perilimbal conjunctiva. Histol Histopathol 2011; 26:323–331.

45   Sun CC, Chiu HT, Lin YF et al. Y-27632, a ROCK inhibitor, promoted limbal epithelial cell proliferation and corneal wound healing. PLoS One 2015;10:e0144571.

46   Fuchs E. The tortoise and the hair: Slow-cycling cells in the stem cell race. Cell 2009; 137:811–819.

47   Dua HS, Azuara-Blanco A. Limbal stem cells of the corneal epithelium. Surv Ophthalmol 2000;44:415–425.

48   Mii S, Murakumo Y, Asai N et al. Epidermal hyperplasia and appendage abnormalities in mice lacking CD109. Am J Pathol 2012;181: 1180–1189.

49   Li J, Xin J, Zhang L et al. Human hepatic progenitor cells express hematopoietic cell markers CD45 and CD109. Int J Med Sci 2014; 11:65–79.

50   Murray LJ, Bruno E, Uchida N et al. CD109 is expressed on a subpopulation of CD34+ cells enriched in hematopoietic stem and progenitor cells. Exp Hematol 1999;27: 1282–1294.

51   Zhang JM, Murakumo Y, Hagiwara S et al. CD109 attenuates TGF-beta1 signaling and enhances EGF signaling in SK-MG-1

human glioblastoma cells. Biochem Biophys Res Commun 2015;459:252–258.

52   Hagiwara S, Murakumo Y, Mii S et al. Processing of CD109 by furin and its role in the regulation of TGF-beta signaling. Oncogene 2010;29:2181–2191.

53   Finnson KW, Tam BY, Liu K et al. Identification of CD109 as part of the TGF-beta receptor system in human keratinocytes. FASEB J 2006;20:1525–1527.

54   Chen Z, Li DQ, Tong L et al. Targeted inhibition of p57 and p15 blocks transforming growth factor beta-inhibited proliferation of primary cultured human limbal epithelial cells. Mol Vis 2006;12:983–994.

55   Meyer-Blazejewska EA, Kruse FE, Bitterer K et al. Preservation of the limbal stem cell phenotype by appropriate culture techniques. Invest Ophthalmol Vis Sci 2010; 51:765–774.

56   Rosenblum MD, Woodliff JE, Madsen NA et al. Characterization of CD 200-receptor expression in the murine epidermis. J Invest Dermatol 2005;125:1130–1138.

57   Kloepper JE, Tiede S, Brinckmann J et al. Immunophenotyping of the human bulge region: The quest to define useful in situ markers for human epithelial hair follicle stem cells and their niche. Exp Dermatol 2008;17:592–609.

58   Ohyama M, Kobayashi T. Isolation and characterization of stem cell-enriched human and canine hair follicle keratinocytes. Methods Mol Biol 2012;879:389–401.

59   Matsue H. CD 200-mediated regulation of skin immunity. J Invest Dermatol 2005; 125:x–xi.

60   Meyer KC, Klatte JE, Dinh HV et al. Evidence that the bulge region is a site of relative immune privilege in human hair follicles. Br J Dermatol 2008;159: 1077–1085.

61   Paus R, Ito N, Takigawa M et al. The hair follicle and immune privilege. J Investig Dermatol Symp Proc 2003;8:188–194.

62   Rosenblum MD, Yancey KB, Olasz EB et al. CD200, a "no danger" signal for hair follicles. J Dermatol Sci 2006;41:165–174.

63   Gorczynski RM, Cattral MS, Chen Z et al. An immunoadhesin incorporating the molecule OX-2 is a potent immunosuppressant that prolongs allo- and xenograft survival. J Immunol 1999;163:1654–1660.

64   Gorczynski R, Chen Z, Khatri I et al. sCD200 present in mice receiving cardiac and skin allografts causes immunosuppression in vitro and induces Tregs. Transplantation 2013;95:442–447.

65   Zhang SS, Huang ZW, Li LX et al. Identification of CD200+ colorectal cancer stem cells and their gene expression profile. Oncol Rep 2016;36:2252–2260.

66   Cheong YK, Ngoh ZX, Peh GS et al. Identification of cell surface markers glypican-4 and CD200 that differentiate human corneal endothelium from stromal fibroblasts. Invest Ophthalmol Vis Sci 2013; 54:4538–4547.

67   Umemoto T, Yamato M, Nishida K et al. Limbal epithelial side-population cells have stem cell-like properties including quiescent state. Stem Cells (Dayton, Ohio) 2006;24: 86–94.

68 Richardson A, Lobo EP, Delic NC et al. Keratin-14-positive precursor cells spawn a population of migratory corneal epithelia that maintain tissue mass throughout life. Stem Cell Reports 2017;9: 1081–1096.

69 Eghtedari Y, Richardson A, Mai K et al. Keratin 14 expression in epithelial progenitor cells of the developing human cornea. Stem Cells Dev 2016;25:699–711.

70 Lopez-Paniagua M, Nieto-Miguel T, de la Mata A et al. Comparison of functional limbal epithelial stem cell isolation methods. Exp Eye Res 2016;146:83–94.

71 Chen B, Mi S, Wright B et al. Investigation of K14/K5 as a stem cell marker in the limbal region of the bovine cornea. PLoS One 2010;5:e13192.

See www.StemCells.com for supporting information available online.